

**Lunar Reconnaissance Orbiter Topographic Mapping Using Leica
Photogrammetry Suite**

A Technical Paper

Presented in Partial Fulfillment of the Requirements for the Degree Master of Science in
the Graduate School of The Ohio State University

Department of Civil and Environmental Engineering and Geodetic Science

By
Li Yang
The Ohio State University
2009

Master's Examination Committee:
Dr. Rongxing Li, Advisor
Dr. Alan Saalfeld

Approved by:

ABSTRACT

The Mapping and Geographic Information Science (GIS) Lab at The Ohio State University (OSU) has been extensively involved with the Lunar Reconnaissance Orbiter (LRO) project since the beginning of its mission. The Lunar Reconnaissance Orbiter is the first mission in NASA's Vision for Space Exploration, a plan to return to the moon and then to travel to Mars and beyond. One of the LRO objectives is to provide the first high-accuracy 3D lunar cartographic maps along with an assessment of potential landing sites for future lunar landed missions at a high level of precision (submeter) (Tooley, C., 2006). For candidate landing sites of future lunar landed missions and other areas of scientific interest, topographic products (such as Digital Elevation Models (DEM), ortho maps, slope maps and special products, VRML data sets, and 3D surface feature measurements) will be produced.

During LRO mission operations, the topographic products generated by the Mapping and GIS lab in this project will directly contribute to assessment and selection of potential landing sites for future landed mission. The Mapping and GIS lab has automated software to generate Digital Terrain Model (DTM) grid points. However, there are some mismatched points in these DTM grid points. So the process of LRO high-precision topographic products still needs some manual operations for editing grid points.

The goal of this paper is to provide the method of importing the DTM grid points generated by the OSU Orbital Mapper software into Leica Photogrammetry Suite (LPS), which could provide terrain editing functions for final high accuracy topographic

products. In this paper, we perform the terrain editing work on the overlap area of NAC images M102064759 and M102057602, which are 50 km long and 7 km wide. The terrain editing process eliminates the mismatched grid points in the DTM grid points generated by the OSU Orbital Mapper software and adds grid points for some terrain areas where do not have grid points in the automatically DTM generation.

The paper is organized in several aspects: 1) introduces LRO Mission, relevant researches in LRO topographic mapping area, OSU Orbital Mapper software, and Leica Photogrammetry Suite; 2) describes the geometric model of Lunar Reconnaissance Orbiter Camera (LROC) Narrow Angle Camera (NAC); 3) describes the workflow of Importing the DTM grid points generated by OSU Orbital Mapper software into LPS; 4) describes the terrain editing process and its results; 5) evaluates the terrain editing work in LPS.

Chapter 1: Introduction

1.1 Lunar Reconnaissance Orbiter Mission

On June 18, 2009, The Lunar Reconnaissance Orbiter and Lunar Crater Observation and Sensing Satellite were launched. LRO is scheduled for a one-year exploration mission at a polar orbit of about 50 kilometers, to create a comprehensive map of the moon's features and resources for future human or robotic landed missions (NASA 2007). The LRO payload, comprised of six instruments and one technology demonstration, will provide key data sets for future missions (NASA 2007). Among LRO's six instruments, the LROC acquires high-resolution images to facilitate safety analysis for potential lunar landing sites and polar illumination characterization (G. Chin et al. 2007).

The LROC Science Operations Center (SOC) is located at Arizona State University where daily uplink and downlink operations take place. U.S. Geological Survey (USGS) Integrated Software for Imagers and Spectrometers (ISIS) package is used for radiometric and geometric processing in the LRO mission. Different versions of LROC data, such as raw, calibrated, and mosaicked versions, are disseminated via website (G. Chin et al. 2007).

In the LRO mission, the Mapping and GIS lab at OSU uses LROC NAC images to do stereo mapping and produce high-accuracy 3D lunar topographic products. The Mapping and GIS lab has developed its own software, OSU Orbital Mapper software, to process LROC NAC images to produce DTM grid points and orthophotos. The Mapping and GIS lab uses the LPS to edit the DTM grid points and generate the 3D surface from the DTM

grid points. Topography information about the lunar surface is essential to assessment and selection of landing sites to ensure safe landings as well as improve surface operations after landing. The developed accurate photogrammetric processing model and integrated mapping products will be critical tools for supporting topographic characterization of landing sites and their assessment and selection for future human or robotic landed missions. In particular, topographic products can provide detailed information about visible ground features and hazards (e.g., big slopes, rocks, craters, etc.) as well as rock abundance within the landing ellipse of a selected landing site.

1.2 Relevant Researches Review

For LRO 3D topographic mapping, the stereo LROC NAC images are used to produce high-precision topographic information. Currently, there are several ways to produce high-accuracy 3D lunar topographic products in the LRO mission. For example, OSU uses OSU Orbital Mapper software to generate dense grid points and use LPS to manually edit these grid points, and then interpolate these grid points to get a surface. On the other hand, Arizona State University uses ISIS to radiometrically calibrate the LROC NAC images, and then import the stereo pair images, the NAC camera model, and spacecraft information into SOCET SET to produce Digital Elevation Models (DEM) of lunar surface (LROC team, 2009).

ISIS is an image processing software package developed at USGS to manipulate imagery collected by current and past NASA planetary missions, including the Lunar Reconnaissance Orbiter (LRO). Isis 3 has specific applications in the LRO mission. For

instance, Ironac2isis program imports an LROC NAC image as an Isis cube containing the image data, and Ironaccal program performs radiometric corrections to an LROC NAC image (USGS Isis, 2009).

BAE Systems' SOCET SET, a digital photogrammetry software application, is used to produce DEM of the lunar surface in the LRO mission. Before using SOCET SET to process the stereo image pair, the images need to be enhanced or corrected in ISIS (Rosiek, 2000). With the input of the stereo pair images, the NAC camera model, and spacecraft information, SOCET SET will run a triangulation process. After the program finishes triangulation with a low RMS error, DEM extraction could begin (LROC team, 2009).

1.3 OSU Orbital Mapper Software

The Mapping and GIS lab has developed the OSU Orbital Mapper software to process LROC NAC images based on rigorous photogrammetric modeling of the imaging geometries to generate DTM grid points. The OSU Orbital Mapper software employs a hierarchical process for stereo matching and tie-point selection from LROC images. The hierarchical process starts with the images of lowest resolution, and then transfers the results to the next higher level to extract and match more interest points (Li al. 2008). After the grid point matching, dense grid points are produced. The dense grid points generated by the OSU Orbital Mapper software have some mismatched grid points, so we need some manual operations for terrain editing to eliminate them. And there are some small and smooth terrain areas that do not have any grid points, so we need to manually

add them on these areas. Over all, we need to improve the accuracy of the DTM grid points by terrain editing.

1.4 Leica Photogrammetry Suite

Leica Photogrammetry Suite, commercial software produced by ERDAS, provides LPS Terrain Editor tool for visualization, check and editing of Digital Terrain Models (DTMs) (ERDAS, Inc., 2009). Terrain Editing is an important work for quality control and improving DTMs. LPS Terrain Editor combines with LPS Stereo allows user to edit the grid points in a stereo environment to obtain maximum accuracy and efficiency. Full 3D stereo imagery can be viewed using either passive polarized or active LCD stereoscopic viewing systems (ERDAS, Inc. 2009). Stereo-enabled graphics cards are also needed to view three-dimensional stereo. As ERDAS recommended, we use the Planar's SD2020 Stereo/3D Monitor and NVIDIA Quadro FX 4600 Stereo-enabled graphics card for LPS stereo display.

From the Planar SD2020 Stereoscopic Monitor User's Guide, we know that the Planar SD2020 uses StereoMirror technology to provide the highest quality stereoscopic image. The Planar SD2020 is composed of two LCD monitors in an up/down configuration separated at a 110-degree angle. A semitransparent mirror is positioned at a bisecting angle between the two monitors. When the user wears the polarizing glasses, the left eye polarized lens of the glasses blocks light from the top monitor while light from the lower monitor is blocked by the right eye lens. The user only sees the left eye image with the eyepiece having the 0°-oriented polarizer and the right eye image with the eyepiece

having the 90° polarizer. Light with a perpendicular polarization is not transmitted, so we can obtain a single, fused stereoscopic image (Planar Systems, Inc. 2006).

LPS Stereo has OpenGL stereo support, so we can view three-dimensional stereo in LPS with proper OpenGL stereo setting in the stereo graphics card. We need to turn on the stereo and use nView clone mode in the NVIDIA Quadro FX 4600 Stereo-enabled graphics card setting.

Once the LPS Stereo setting finishes, we could see the 3D visualization of the terrain in the LPS Terrain Editor. In the 3D visualization, we could check whether or not the grid points are on the surface of the terrain during the terrain editing process. LPS Stereo combines with LPS Terrain Editor enables us to zoom in or zoom out the stereo image continuously and discretely. We could also measure the elevation difference between the grid points and the terrain surface. Over all, LPS Stereo provides user with a comfortable feeling when doing terrain editing work and improve the accuracy of the editing work.

Chapter 2: Geometric Model of LROC NAC

2.1 Introduction of LROC NAC

The LROC has two narrow-angle cameras to provide 0.5 m scale panchromatic images over a 5 km swath at 50 kilometers altitude (G. Chin et al. 2007). The focal length of each NAC is about 700 mm and the cross-track field-of-view (FOV) is about 2.85°. Table 1 lists the NAC specifications (Bowman-Cisneros et al., 2009).

Table 1 - NAC specifications (Bowman-Cisneros et al., 2009)

	NAC-L	NAC-R
FOV	2.8502°	2.8412°
IFOV	10.0042 μ rad	9.9764 μ rad
Image scale at 50 km altitude	0.5 m/pixel	
Maximum image size at 50 km altitude	2.49 x 26 km	2.48 x 26.1 km
f/# (Ritchey-Chretien)	3.577	3.590
Effective focal length	699.62 \pm 0.08 mm	701.57 \pm 0.09 mm
Distortion coefficient	0.0000181 \pm 0.0000005	0.0000183 \pm 0.0000005
Optical center location	sample 2548 \pm 8	sample 2568 \pm 8
Primary mirror diameter	198 mm	
MTF (Nyquist)	0.23	
Gain	90.5 \pm 2.6 e-/DN	92.5 \pm 1.5 e-/DN
Noise	101 \pm 7 e-	97 \pm 2 e-
Detector Fullwell	334,000 \pm 31,000 e-	352,000 \pm 4100 e-
SNR (400-750 nm)	> 52	> 49
Detector digitization	12-bit, encoded to 8-bits	
Lossless compression ratio	1.7:1	

Structure + baffle	Graphite-cyanate composite
Detector	Kodak KLI-5001G
Pixel format	1 x 5,064*
Analog/digital converter	Honeywell ADC9225
FPGA	Actel RT54SX32-S
Voltage	28 ± 7V DC
Peak power	9.3 W
Orbit average power	6.4 W
Mass (both NACs)	16.4 kg
Volume (length x diameter)	118 cm x 27 cm (incl. radiator)

* Of the 5064 pixels, 39 masked pixels on the right and 21 masked pixels on the left are used for dark reference.

Bowman-Cisneros et al. (2009) mentioned that the CCDs of the NACs are perpendicular to the spacecraft's X-axis. They also reported that pixel 0 for the NAC-L is at the -Y end of its CCD and pixel 0 for the NAC-R is at the +Y end of its CCD (in spacecraft coordinates). In order to obtain both images have the same ground orientation, one of the NAC frames from a NAC-L and NAC-R paired observation must be transformed.

In the LRO mission, the stereo LROC NAC images, which are mainly obtained by re-imaging the same area during repeated orbits, are used to produce high-precision topographic products.

2.2 Geometric Modeling of LROC NAC Sensor

LROC NAC sensor uses a generic linear scanning (push-broom) sensor model, whose conceptual configuration is shown in Figure 1.

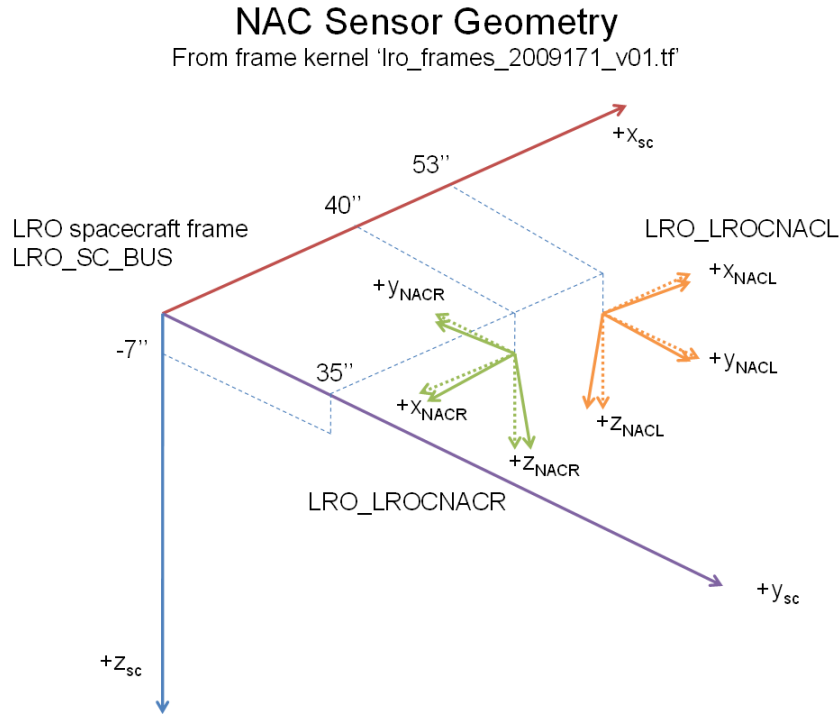


Figure 1 - LROC NAC sensor geometry

In LROC NAC sensor models, the relationship of a 3D ground point (X_p, Y_p, Z_p) and its corresponding image coordinates (x_p, y_p) is represented by the collinearity equation (Wolf, 1983):

$$x_p = -f \frac{m_{11}(X_p - X_S) + m_{12}(Y_p - Y_S) + m_{13}(Z_p - Z_S)}{m_{31}(X_p - X_S) + m_{32}(Y_p - Y_S) + m_{33}(Z_p - Z_S)}$$

$$y_p = -f \frac{m_{21}(X_p - X_S) + m_{22}(Y_p - Y_S) + m_{23}(Z_p - Z_S)}{m_{31}(X_p - X_S) + m_{32}(Y_p - Y_S) + m_{33}(Z_p - Z_S)} \quad (1)$$

where (X_S, Y_S, Z_S) are the coordinates of the camera center in object space, f is the focal

length of the camera, and m_{ij} are the elements of a rotation matrix that is determined entirely by three rotation angles (ω , ϕ , κ) from the image space to the object space.

$$\begin{aligned}
m_{11} &= \cos \phi \cos \kappa \\
m_{12} &= \sin \omega \sin \phi \cos \kappa + \cos \omega \sin \kappa \\
m_{13} &= -\cos \omega \sin \phi \cos \kappa + \sin \omega \sin \kappa \\
m_{21} &= -\cos \phi \sin \kappa \\
m_{22} &= -\sin \omega \sin \phi \sin \kappa + \cos \omega \cos \kappa \\
m_{23} &= \cos \omega \sin \phi \sin \kappa + \sin \omega \cos \kappa \\
m_{31} &= \sin \phi \\
m_{32} &= -\sin \omega \cos \phi \\
m_{33} &= \cos \omega \cos \phi
\end{aligned} \tag{2}$$

The variables (X_S , Y_S , Z_S , ω , ϕ , κ) are called the exterior orientation (EO) parameters.

The image coordinates (x_p , y_p) are calculated from the pixel coordinates using principal point position, pixel size, and lens distortion corrections.

For a linear scanning sensor which has one set of EO parameters for each scan line of the image, the EO parameters change along with time (or scan line). Changes of exterior orientation parameters can be modeled by the following polynomials, where t is the imaging time of the scan line; ($X_S^0, Y_S^0, Z_S^0, \phi^0, \omega^0, \kappa^0$) are the EO parameters of a starting line (i.e., the zero-order coefficients of the polynomials); and a_i, \dots, f_i ($i=1, 2, 3$) are the first-, second-, and third-order coefficients of the polynomials (Li et al., 2008).

$$\begin{aligned}
X_s^t &= X_s^0 + a_1 t + a_2 t^2 + a_3 t^3 \\
Y_s^t &= Y_s^0 + b_1 t + b_2 t^2 + b_3 t^3 \\
Z_s^t &= Z_s^0 + c_1 t + c_2 t^2 + c_3 t^3 \\
\varphi^t &= \varphi^0 + d_1 t + d_2 t^2 + d_3 t^3 \\
\omega^t &= \omega^0 + e_1 t + e_2 t^2 + e_3 t^3 \\
\kappa^t &= \kappa^0 + f_1 t + f_2 t^2 + f_3 t^3
\end{aligned} \tag{3}$$

In a photogrammetric adjustment, solving polynomial coefficients instead of the exterior orientation parameters of each scan line greatly reduces the computational complexity while still achieving a high level of accuracy (Li et al., 2002b).

LRO acquires stereo images by re-imaging the same area from different orbits that form a convergence angle for stereo measurement. Bundle adjustment of stereo LROC images provides consistent and high precision EO parameters of the images, which are essential for high precision 3D mapping.

Chapter 3: Importing the DTM Grid Points Generated by the OSU Orbital Mapper Software into LPS

3.1 Background

In this paper, we process the LROC NAC stereo images, NAC images M102064759 and M102057602, taken during LRO orbit 193, near the Apollo 16 landing site. The whole overlap area of these two images is about 50 km long and 7 km wide. The latitude of the overlap area is $8^{\circ} \text{ S} \sim 10^{\circ} \text{ S}$ and the longitude of the overlap area is $15.2^{\circ} \text{ E} \sim 15.5^{\circ} \text{ E}$ (LROC team, 2009).

Using the OSU Orbital Mapper Software, we could perform LRO topographic mapping of these two stereo images. There are five stages for LRO topographic mapping. The first step is to process the individual LROC NAC image of the stereo image pair. The software converts LROC NAC .img file to .bmp file, constructs an image pyramid of five levels based on the original images by sub-sampling of each previous level of images at one-half of that level's scale, and generates interest points. The second step is to match the interest points for the stereo images. Tie points between the stereo images were selected from the set of matched interest points will be used in the subsequent bundle adjustment. The third step is to perform bundle adjustment to generate refined EO parameters. The refined exterior orientation data generated in bundle adjustment will be used for grid points matching. The fourth step is grid points matching. Dense grid points with spacing of 3 pixels are defined and matched in the original images. The grid-point matching is controlled by Delaunay triangles that are formed by the previously matched interest points. This method has been successfully used in dense matching of rover images for

rock extraction, modeling and matching (Li et al., 2007a). The final step is to produce dense grid points with 3 pixels grid spacing.

The dense grid points generated by OSU Orbital Mapper Software have inaccurate points in some areas. So we import them into LPS to perform terrain editing process to eliminate inaccurate grid points and add more grid points to improve the accuracy of the final products. Since LPS do not have a well-defined LROC NAC model, we need to define the LROC NAC model in the LPS. Though we have done bundle adjustment in OSU Orbital Mapper Software, LPS does not allow us to directly import the bundle adjusted EO parameters into LPS. Therefore, we need to redo the bundle adjustment in LPS.

In a word, we need five steps to import the dense grid points generated by the OSU Orbital Mapper Software into LPS (Figure 2). The following sections will discuss the five steps in detail.

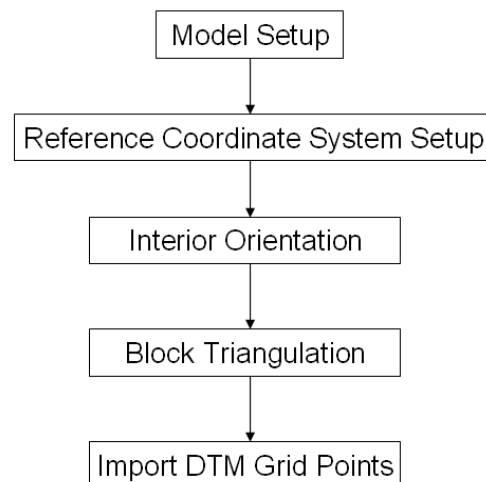


Figure 2 - The workflow of importing the dense grid points generated by the OSU Orbital Mapper Software into LPS

3.2 Model Setup in LPS

In order to process the LROC NAC images, we need to define an appropriate sensor model for LROC NAC in LPS. As mentioned in section 2.2, LROC NAC sensor uses a generic linear scanning (push-broom) sensor model and uses third-order polynomials model for data processing, we select a “Generic Pushbroom” Geometric Model in “Polynomial-based Pushbroom” Geometric Model Category for model setup (Figure 3).

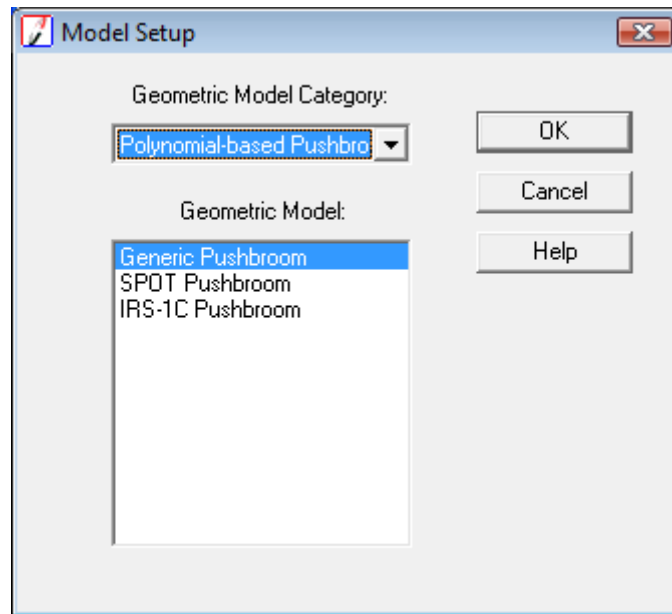


Figure 3 - Model Setup Dialog

3.3 Reference Coordinate System Setup in LPS

We need to define the projection, spheroid, and datum for the block project. We define an equidistant cylindrical projection on the moon spheroid datum for processing LROC NAC images in LPS (Figure 4). We also define specific information about the equidistant cylindrical projection, such as the latitude of standard parallel, the longitude of central meridian, and false easting and false northing (Figure 5).

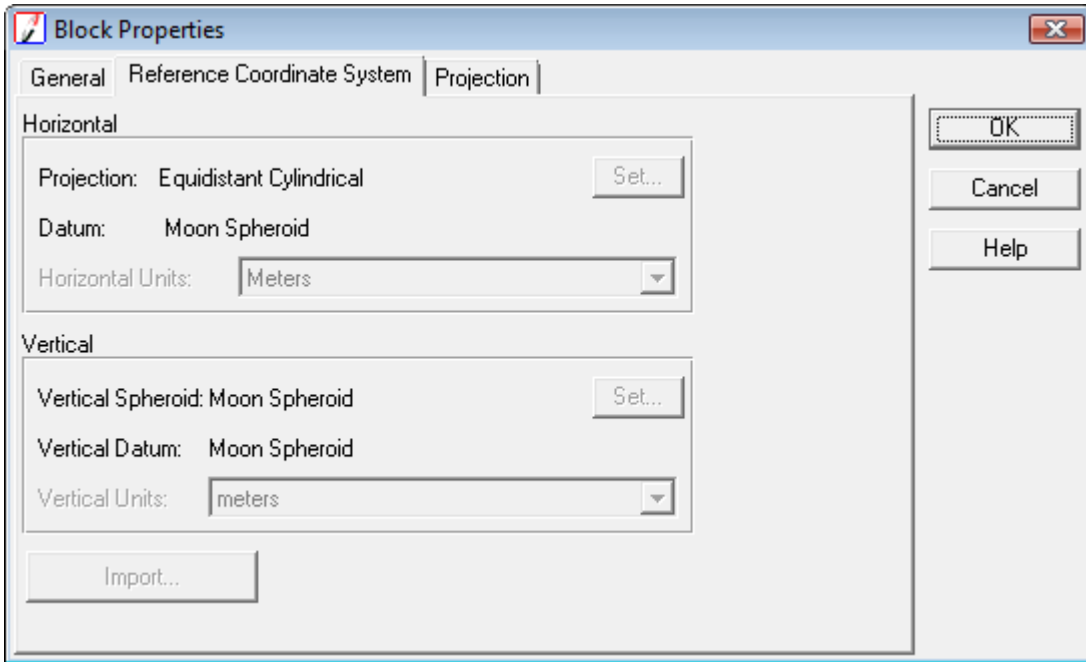


Figure 4 - Reference Coordinate System Setup

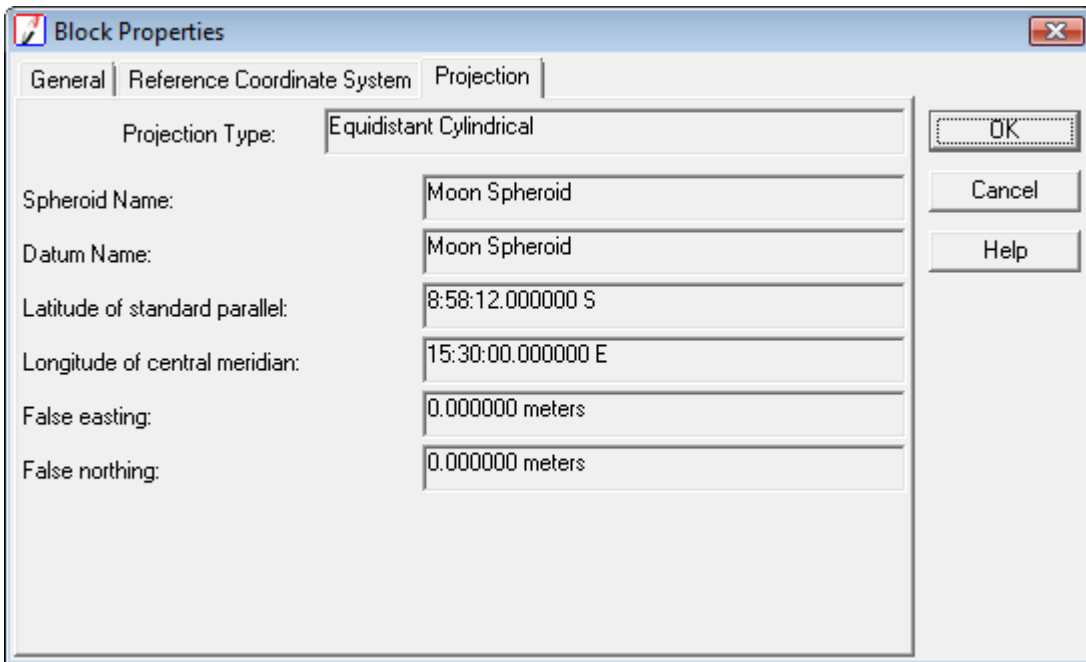


Figure 5 - Projection Setup

3.4 Interior Orientation

- 1) Define specific LROC NAC model information

All the parameters associated with a specific LROC NAC sensor model (i.e. NAC-L and NAC-R) from given sensor model information should be defined in LPS. So the focal length of the sensor, principal point coordinates, pixel size of sensor, and the number of columns in the image should be specified (Figure 6 and Figure 7).

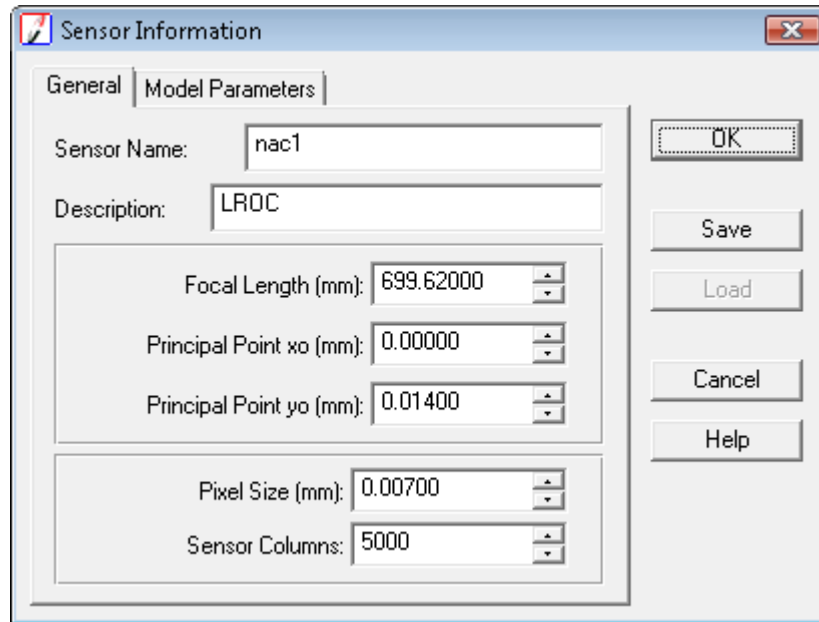


Figure 6 – Specific LROC NAC-L sensor model defined in LPS

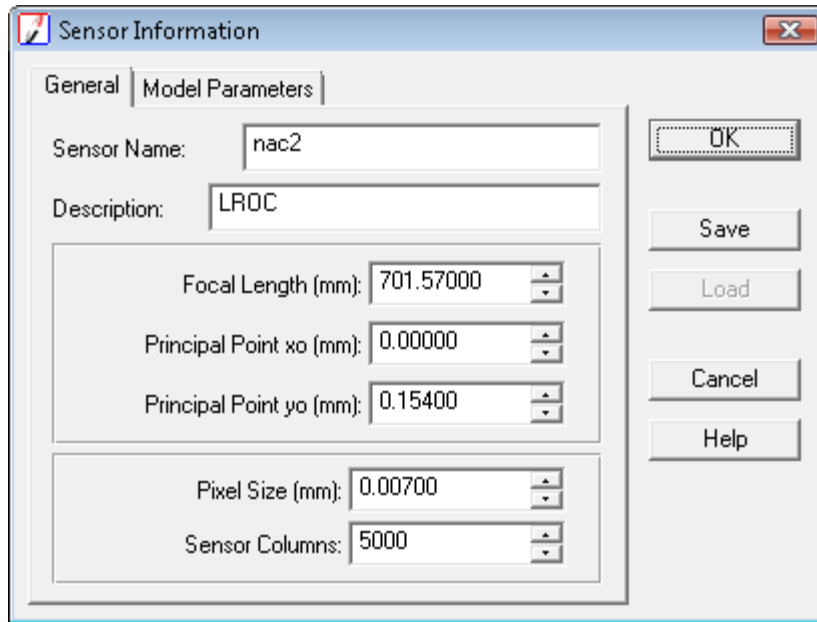


Figure 7 – Specific LROC NAC-R sensor model defined in LPS

The polynomial orders to be used during the triangulation process also should be specified. For the LROC NAC sensor model, the third-order polynomial is used during the triangulation process (Figure 8).

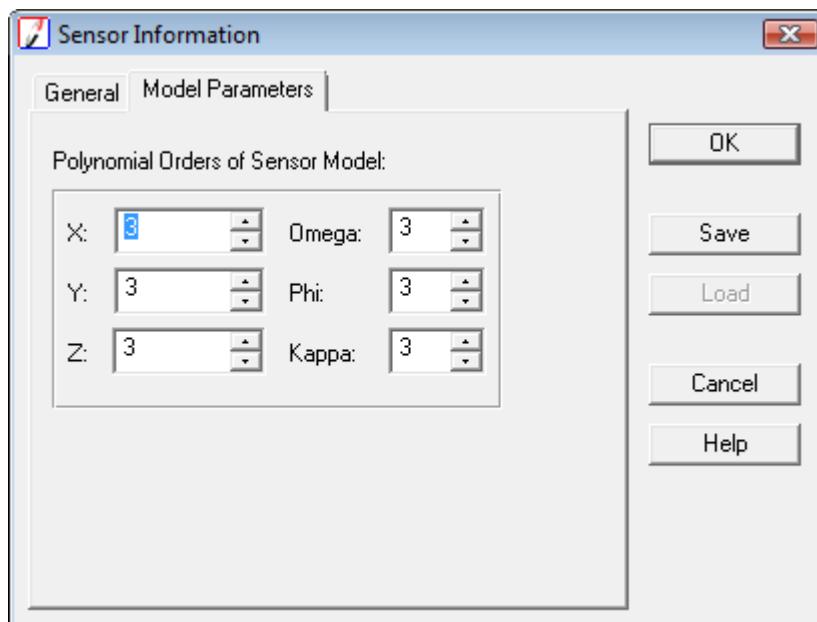


Figure 8 – Model Parameters for LROC NAC sensor model

2) Define specific frame attributes information

The specific frame information for the LROC NAC image should be defined in LPS (Figure 9). These attributes are the side incidence angle, the track incidence angle, the ground resolution (meters), and whether the sensor line is along the x or y axis. The side incidence angle is the angle between the vertical position of the satellite and the side viewing direction of the satellite when the sensor is scanning along the side. The track incidence angle is the angle between the vertical position of the satellite and the forward or backward viewing direction of the satellite when the sensor is scanning along the direction of flight. The sensor line defines the direction of the scan line which is used by the satellite to record the data (ERDAS, Inc. 2009).

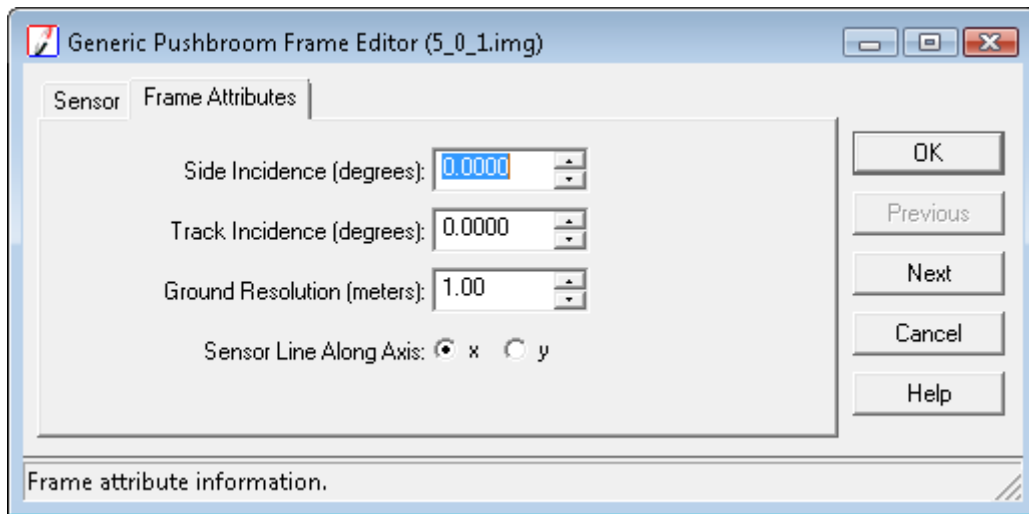


Figure 9 – Specific frame attributes information defined in LPS

3.5 Block Triangulation

LPS Project Manager uses bundle block adjustment techniques for block triangulation. Since LPS does not allow us to directly import the refined EO parameters which are generated in the bundle adjustment in the OSU Orbital Mapper Software into LPS, we

need to redo the bundle adjustment in LPS. LPS supports several ways of obtaining control points for block triangulation. For example, we could use the classic point measurement tool to manually select control points in LPS. We could also use the refined EO parameters and image coordinates of points to generate their corresponding ground coordinates in the OSU Orbital Mapper Software, and then import both ground coordinates and image coordinates into LPS.

In this paper, we use the classic point measurement tool in the LPS to import the control points generated by the OSU Orbital Mapper Software (Figure 10). We import the ground coordinates of control points as “Reference Points (3D)” and image coordinates of control points as “Image Points only”. The ground coordinates of control points ASCII file should follow the format: Point ID, X, Y, Z. The image coordinates of control points ASCII file should follow the format: Image ID, Point ID, X, Y.

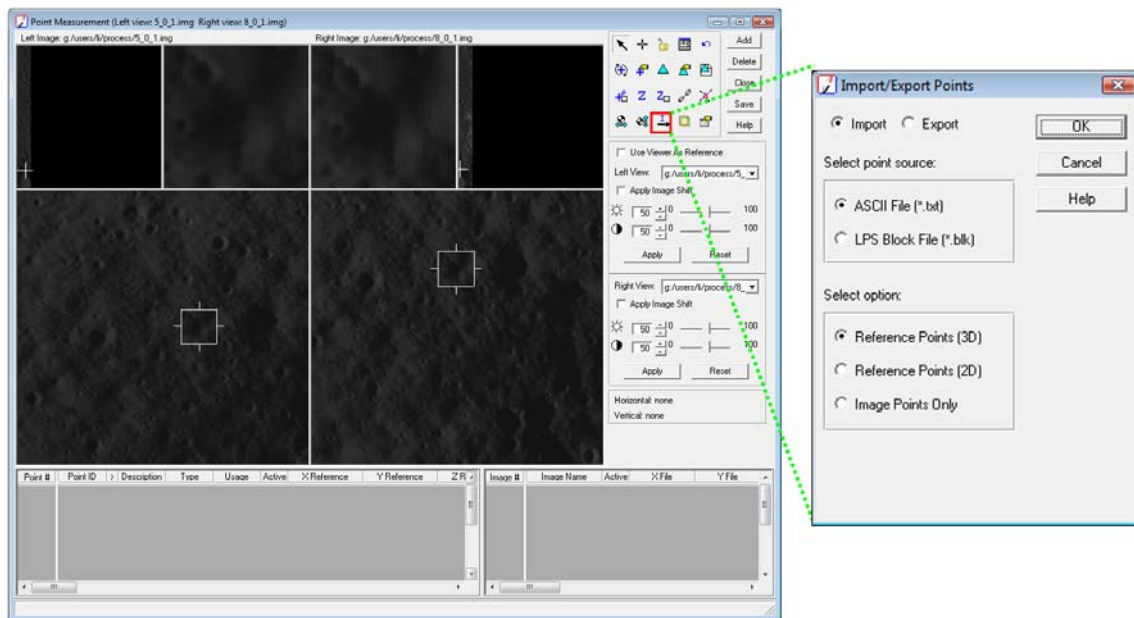


Figure 10 – Importing control points in the classic point measurement tool

In the study, we generated 4244 control points and 2123 check points in the OSU Orbital Mapper Software. We import these 4244 control points and 2123 check points into LPS to redo bundle adjustment. The distribution of 4244 control points and 2123 check points are in the Figure 11. The distribution of control points and check points are important in the bundle adjustment. Uneven distribution of control points may cause the bad quality of the bundle adjustment. Uneven distribution of check points may not reflect the quality of the bundle adjustment very well. From Figure 11, we know that these control points and check points are distributed evenly in the image space.

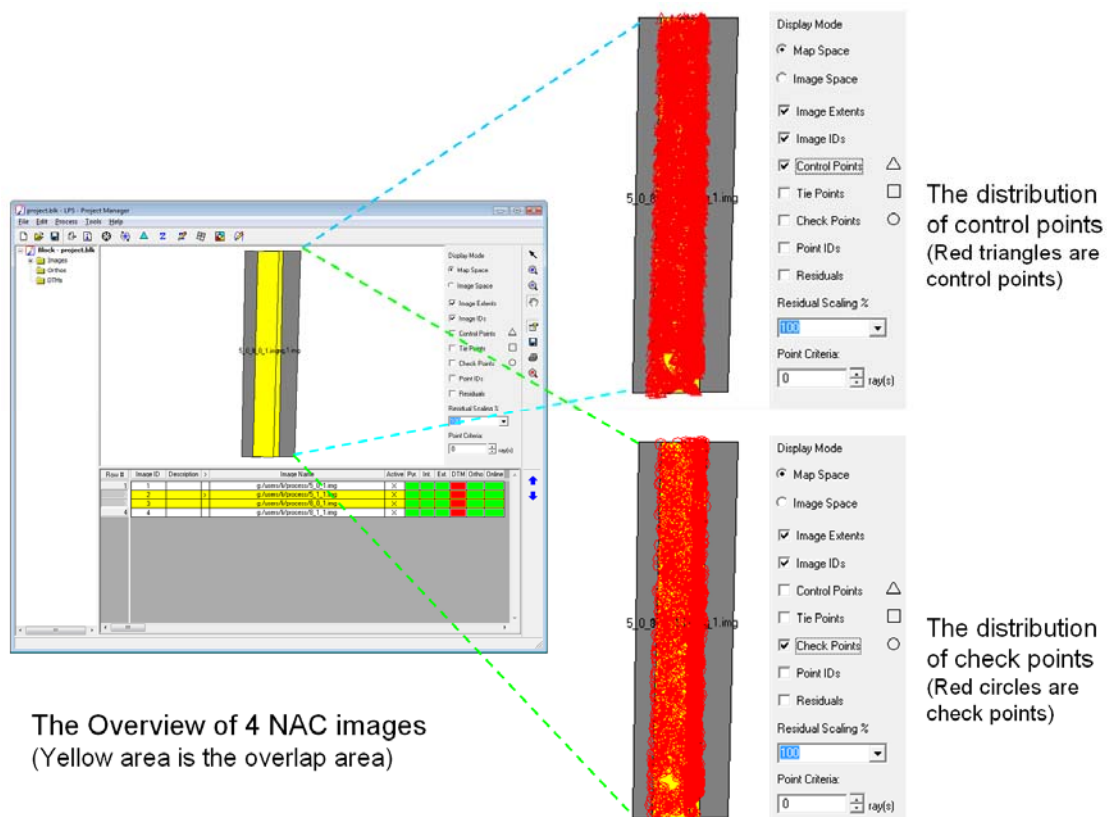


Figure 11 – The distribution of control points and check points in the images

After the triangulation finishes, we need to check the results. At first, we make sure that the triangulation result has converged with a small RMSE value. Then we use check

points to determine the accuracy of the block triangulation. We use the bundle adjusted EO parameter and the ground coordinates of the check points to compute the image coordinates of the check points. The difference between the original image coordinates of the check points and the computed image coordinates of the check points is the image coordinates' residuals of the check points after bundle adjustment. We compare the image coordinates' residuals of these 2123 check points after LPS block triangulation with the image coordinates' residuals of these 2123 check points after the OSU Orbital Mapper Software's bundle adjustment (Table 2). From Table 2, we know that the image coordinates' residuals of these 2123 check points after LPS block triangulation are smaller than the image coordinates' residuals after the OSU Orbital Mapper Software's bundle adjustment. So we can accept the block triangulation result and finish the block triangulation in LPS.

Table 2 - The image coordinates' residuals of 2123 check points after LPS block triangulation compared to the image coordinates' residuals after the OSU Orbital Mapper Software's bundle adjustment

		LPS	OSU Orbital Mapper Software
Image coordinates' residuals in x direction (pixels)	Average Absolute Value	0.003626	0.534683
	Standard Deviation	0.004894	0.297666
Image coordinates' residuals in y direction (pixels)	Average Absolute Value	0.244012	0.36968
	Standard Deviation	0.327881	1.171213

3.6 Import DTM Grid Points into LPS

There are various kinds of terrain data could be imported into LPS to perform terrain editing, such as raster DEM, TINs or GRID DTMs. In the LPS, we can edit the elevation (Z coordinate), but not the XY position of a point in a DEM (digital elevation model) file because a raster DEM always has a regular grid spacing. However, we could edit the XYZ position of a point in a TINs or GRID DTMs.

The DTM grid points generated by OSU Orbital Mapper software are ASCII XYZ file, which recorded the 3D coordinates of the DTM grid points. But LPS does not allow us to import DTM in the format of ASCII XYZ file, the format change of the DTM grid points is necessary. We can change the DTM grid points from ASCII XYZ (*.xyz) to .ltf file by using the Terrain Prep Tool. LTF file format is a kind of Grid DTMs supported in the LPS, which allows us to edit the XYZ position of a point.

Chapter 4: Terrain Editing

4.1 Terrain Editing Process

After the DTM grid points generated by OSU Orbital Mapper software have been imported into LPS, we can use the LPS Terrain Editor to edit them. The LPS Terrain Editor combines with LPS Stereo provide an interactive, stereo-enabled environment for the visualization and editing of terrain data to us. When we edit the terrain data, the original images are loaded as a backdrop in the stereo view. The terrain data can be displayed in different ways to assist us in identifying the quality of them. We usually display the terrain data as mass points and contours in the stereo environment when we check the quality of the DTM grid points (Figure 12). The contour lines could reflect the elevation of mass points. So we can check the quality of the DTM grid points by checking whether or not the contour lines show the topographic information of the terrain.

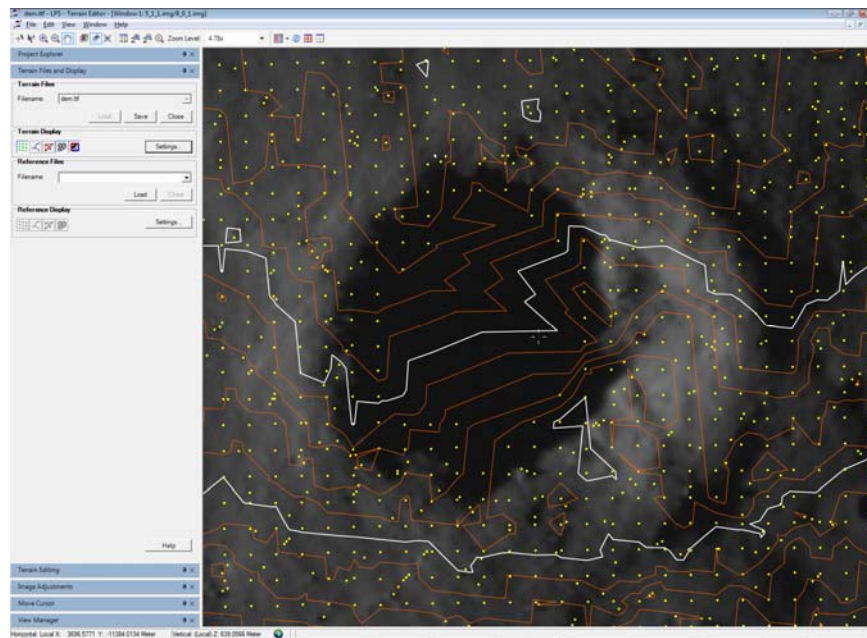


Figure 12 - Terrain data displayed as mass points and contours in the LPS Terrain Editor

The whole terrain editing process includes two parts: deleting inaccurate grid points and adding grid points. At first, we delete the inaccurate points in the original DTM grid points. Then we add more necessary grid points based on the deleting work's results.

The deleting inaccurate grid points' work begins with checking the whole part of grid points one by one. If we find some grid points do not fit the terrain surface well in the 3D visualization, we will delete them. If we find some grid points in the black area in the image, we will delete them too.

After we finish deleting inaccurate grid points' work, we will check the preserved grid points one by one. If we find some areas do not have any grid points, we will add grid points on these areas. When we add the grid points, we should make sure that the cursor is resting on the terrain.

4.2 Terrain Editing Results

We have finished the terrain editing work about the whole overlap area of NAC images M102064759 and M102057602, which are 50 km long and 7 km wide. There are 27642498 original DTM grid points in this area. During the terrain editing process, we have eliminated 73506 grid points and added 10147 grid points (Figure 13). The result will be discussed in the following parts.

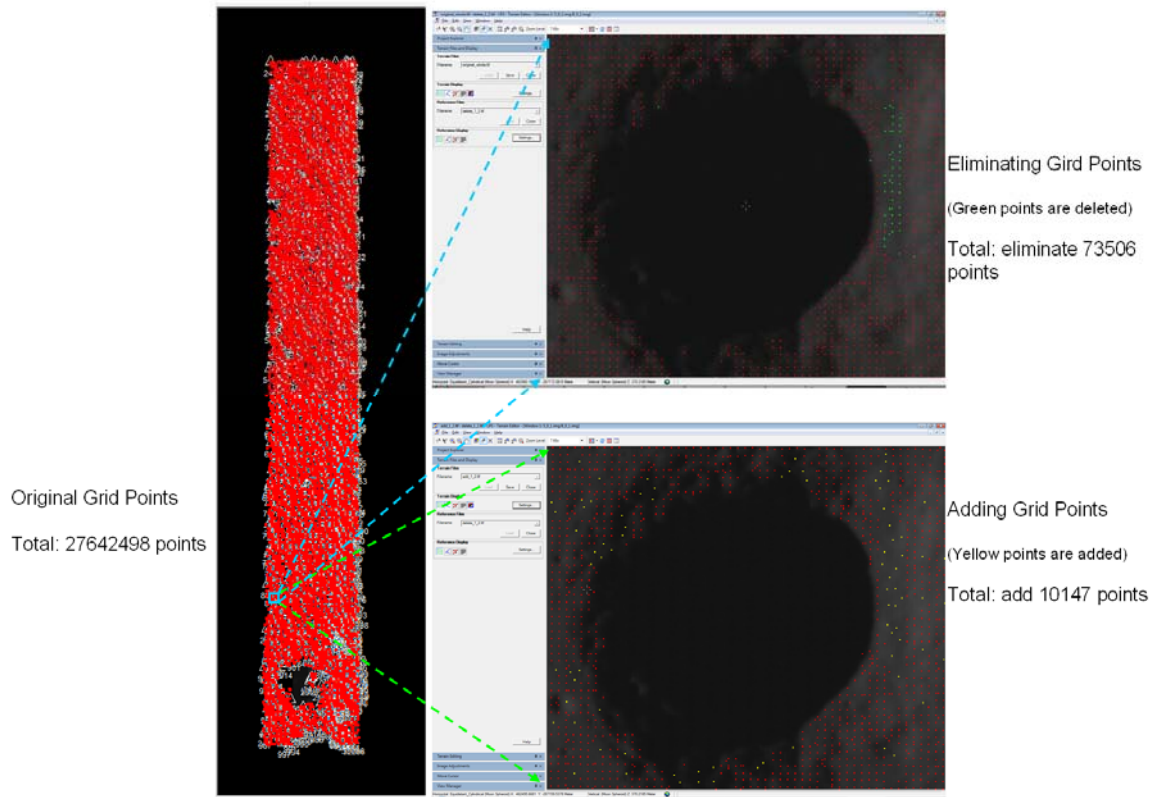


Figure 13 – Terrain editing results

1. Eliminating Grid Points

In the eliminating grid points' work, we have eliminated lots of grid points in the black area (Figure 14). The black areas are the shadowed areas without illumination, so there should not have any points in the black areas. And we have eliminated lots of mismatched points in the big crater's wall (Figure 15).

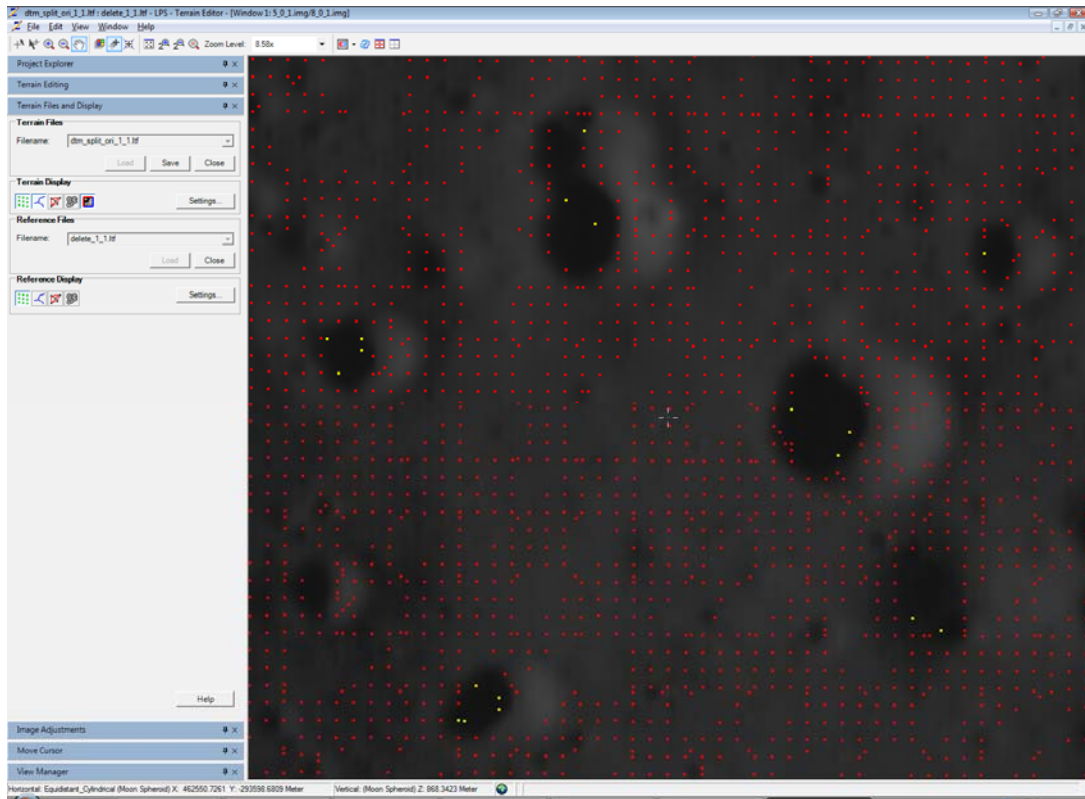


Figure 14 – Wrong grid points deleted in the black area (yellow points are deleted)

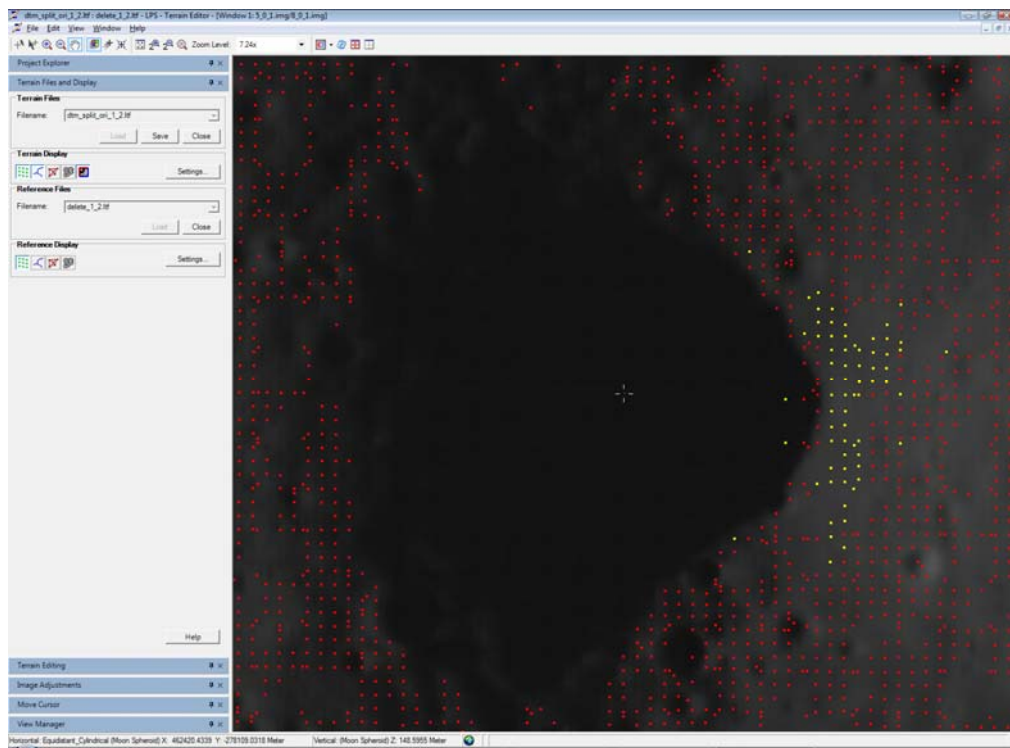


Figure 15 – Wrong grid points deleted in the big crater's wall (yellow points are deleted)

2. Adding Grid Points

In the adding grid points' work, we have added lots of grid points on small smooth terrain areas where there is a lack of sufficient topographic information (Figure 16). And we have added lots of points on the crater wall areas where they do not have enough grid points (Figure 17).

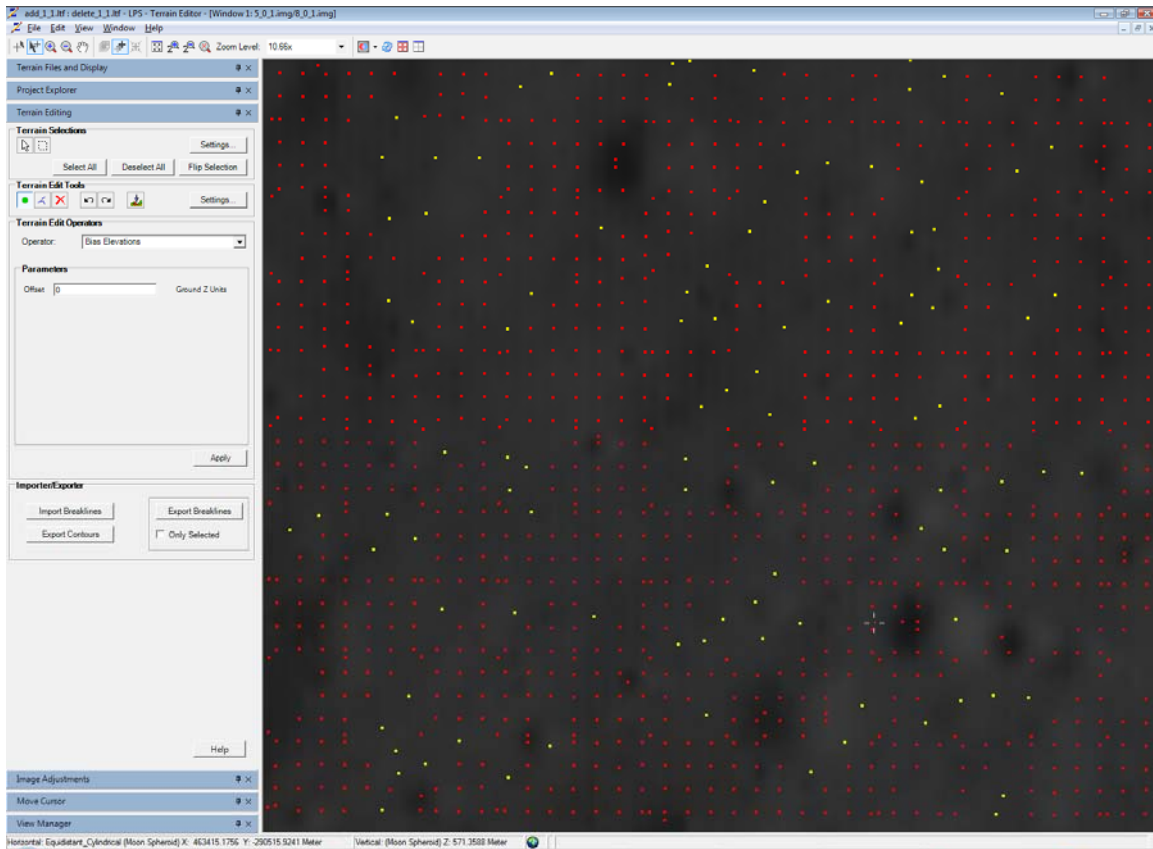


Figure 16 – Grid points added in the smooth area (yellow points are added)

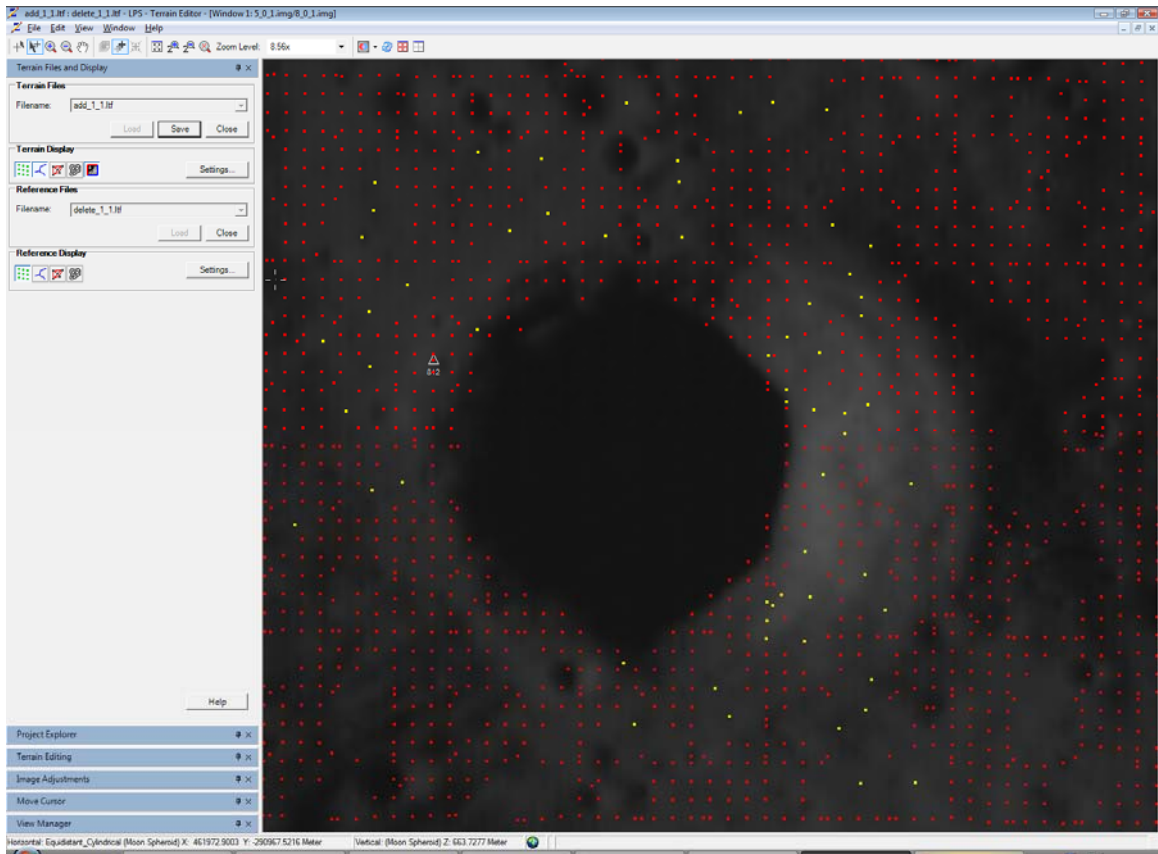


Figure 17 – Grid points added on the crater wall (yellow points are added)

Chapter 5: Evaluation of the Terrain Editing Work in LPS

This chapter evaluates the terrain editing work in LPS by comparing the DEM before terrain editing (Figure 18) with the DEM after terrain editing (Figure 19). These two DEMs with a grid spacing of 3 meters are generated by using Surface DTM in the Terrain Prep Tool.

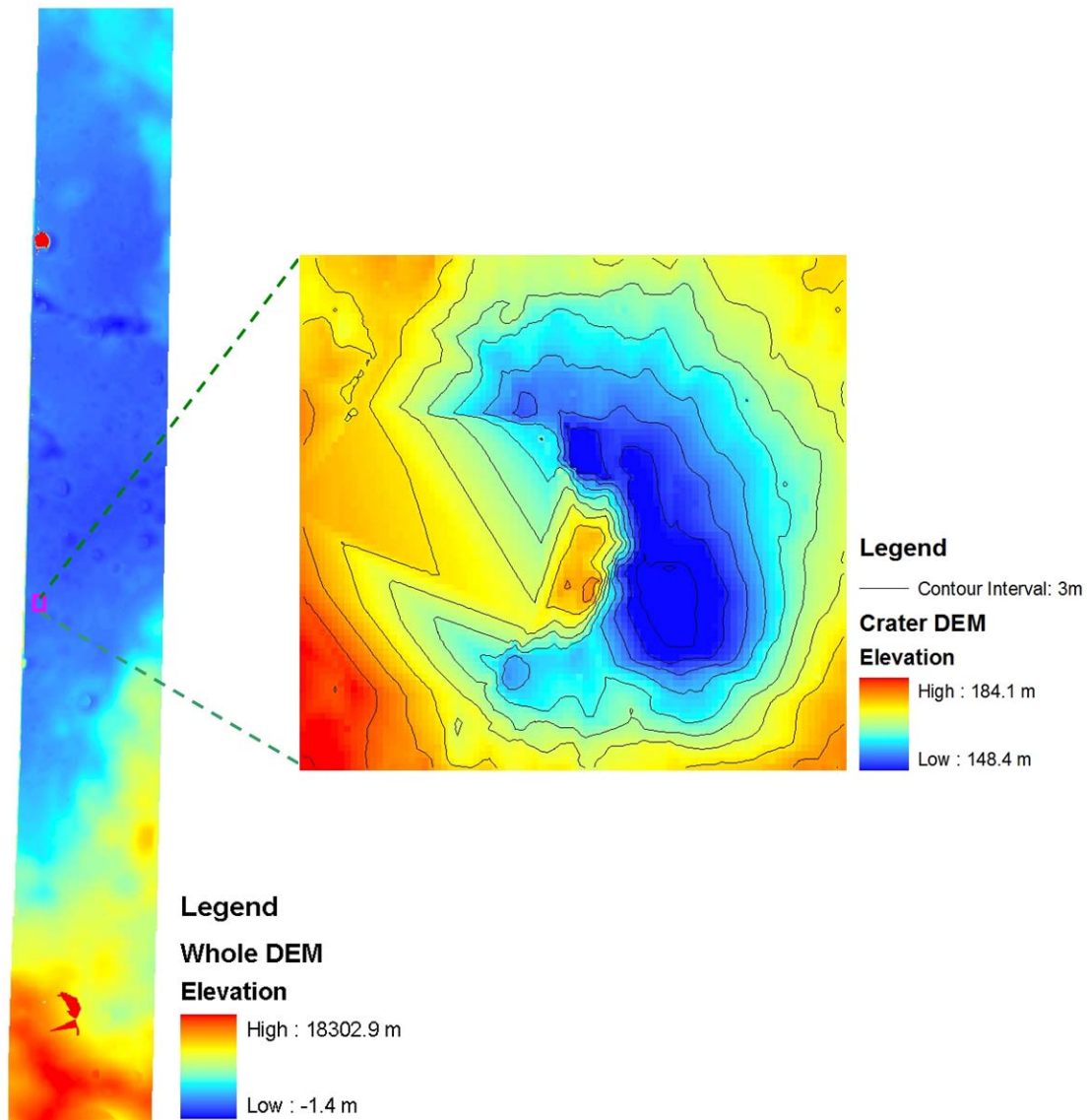


Figure 18 – DEM before terrain editing (Grid spacing: 3 m)

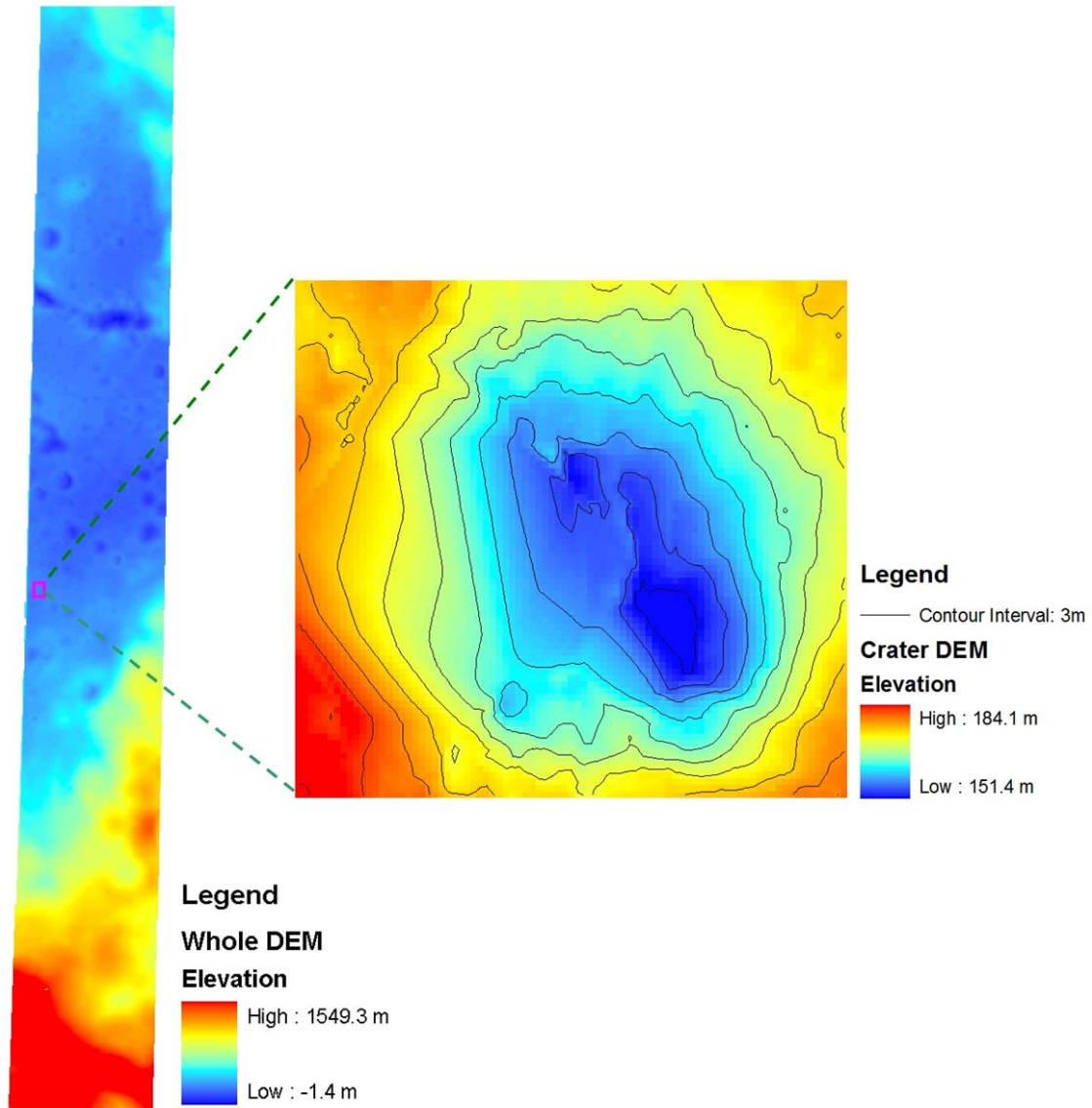


Figure 19 – DEM after terrain editing (Grid spacing: 3 m)

Comparing the elevation of the whole DEM before terrain editing with the whole DEM after terrain editing, we find that the range of the elevation changes too much. There are some terrain areas have blunder before terrain editing. Comparing the small crater's DEM before terrain editing with the one after terrain editing, we can see that terrain editing work improves the topographic information of the crater. In the Figure 17, the left part of

the crater has abnormal contour lines. Looking at the stereo images, we know that this kind of topographic information is wrong. That means there should be a lot of wrong grid points in the left part of the crater which causes these abnormal contour lines. In the Figure 18, the contour lines give us a reasonable outline of the crater and show the proper topographic information of the crater.

Over all, the terrain editing work in the LPS eliminates the inaccurate grid points and adds accurate grid points. The terrain editing work plays an important role in improving the accuracy of the grid points generated by the Mapping and GIS lab's OSU Orbital Mapper software. So the terrain editing function in LPS provides a method to improve the accuracy of topographic products in the LRO mission.

References

1. Batson, R.M., 1987, Digital Cartography of the Planets: New Methods, Its Status, and Its Future, *Photogrammetric Engineering and Remote Sensing*, Vol. 53, No. 9, pp.1211-1218.
2. Batson, R.M. and Eliason, E.M., 1995. Digital Maps of Mars, *Photogrammetric Engineering and Remote Sensing*, Vol. 61, No. 12, pp.1499-1507.
3. Bowman-Cisneros et al., 2009. LROC EDR/CDR Data Product Software Interface Specification.

URL: http://geo.pds.nasa.gov/missions/lro/docs/lroc/lroc_edr_cdr_sis.pdf (last date accessed: Nov. 12, 2009).
4. Chen, Y., J. W. Hwangbo and R. Li 2009. Photogrammetric Processing of Mars HiRISE Imagery for Large Area Topographic Mapping. Abstract (1 page) and presentation, ASPRS 2009 Annual Conference, Baltimore, MD, March 8-13, 2009.
5. Chin, G., Scott Brylow, Marc Foote, James Garvin, Justin Kasper, John Keller, Maxim Litvak, Igor Mitrofanov, David Paige, Keith Raney, Mark Robinson, Anton Sanin, David Smith, Harlan Spence, Paul Spudis, S. Alan Stern and Maria Zuber 2007. Lunar Reconnaissance Orbiter Overview: The Instrument Suite and Mission. *Space Science Reviews*, Vol.129, No. 4, pp. 391–419.
6. ERDAS, Inc. 2009. LPS 9.3 System Specifications.

URL :<http://www.erdas.com/Products/ERDASProductInformation/tabid/84/currentid/1110/default.aspx> (last date accessed: Nov. 12, 2009).
7. Hansen, Thomas P. 1970. Guide to lunar orbiter photographs (NASA SP-242). Washington, Scientific and Technical Information Office, National Aeronautics

- and Space Administration.
8. Houghton, M., C. Tooley, and R. Saylor, Jr., Mission Design and Operations Considerations for NASA's Lunar Reconnaissance Orbiter, IAC-07-C1.7.06.
 9. Keller, J., Gordon Chin and Thomas Morgan 2007. Lunar Reconnaissance Orbiter: Instrument Suite and Objectives. IAC-07-A3.6.A.03.
 10. Lucey, P. G., S. J. Lawrence, M.R. Robinson, B. T. Greenhagen, D.A. Paige, M. B. Wyatt, and A. R. Hendrix 2009. The Compositional Contribution of LRO. Lunar Reconnaissance Orbiter Science Targeting Meeting, 2009.
 11. Stooke, P. J. 2006. Locating Landed Spacecraft and Artificial Impact Craters in LRO Images. Lunar and Planetary Science XXXVII, 2006.
 12. Li, R. Y. Chen, S. He, L. Yang, M. Tang, and the MER Science Team 2009. Rover Localization: Comparison between Bundle Adjustment-based and HiRISE Orbital Image-based Methods. Abstract and Poster. 40th Lunar and Planetary Science Conference, The Woodlands, TX, March 23-27, 2009.
 13. Li, R., K. Di, J. W. Hwangbo, Y. Chen and the Athena Science Team 2008. Rigorous Photogrammetric Processing of HiRISE Stereo Images and Topographic Mapping at Mars Exploration Rovers Landing Sites. Poster and abstract (2 pages) and presentation, 39th Lunar and Planetary Science Conference, League City, TX, March 10–14, 2008.
 14. Li, Ron, Kaichang Di, Ju Won Hwangbo, Yunhang Chen 2007. Rigorous Photogrammetric Processing of HiRISE Stereo Images for Topographic and Geomorphologic Analysis at MER landing sites. Abstract and Poster. AGU Fall Meeting, San Francisco, CA, December 10 – 14, 2007.

15. Li, R., J.W. Hwangbo, Y. Chen and K. Di 2008. Rigorous Photogrammetric Processing of HiRISE Stereo Images for Mars Topographic Mapping. The XXI Congress Beijing, Commission IV, WG IV/7, 1-11 July, Beijing, China, published in the International Archives of the Photogrammetry, Remote Sensing and Spatial Information Sciences, Vol. 37, no. B4-Commission IV, pp. 987-992.
16. Li, R., G. Zhou, N.J. Schmidt, C. Fowler, and G. Tuell, 2002b. Photogrammetric Processing of High-resolution Airborne and Satellite Linear Array Stereo Images for Mapping Applications, International Journal of Remote Sensing, Vol. 23, No. 20, pp. 4451-4473.
17. LROC team, 2009. Digital Elevation Models (DEM).
URL:<http://lroc.sese.asu.edu/news/index.php?/archives/96-Digital-Elevation-Models-DEM.html> (last date accessed: Nov. 12, 2009).
18. NASA, 2007. NASA Facts. URL: <http://lro.gsfc.nasa.gov> (last accessed date: Nov. 12, 2009).
19. Planar Systems, Inc. 2006. Planar SD2020 Stereoscopic Monitor User's Guide, URL:http://www.planar.com/products/docs/CBU/current_manual/mn-planar-sd2020.pdf (last date accessed: Nov. 12, 2009).
20. Robinson, M. S., E. M. Eliason, H. Hiesinger, B. L. Jolliff, A. S. McEwen, M. C. Malin, M. A. Ravine, D. Roberts, P. C. Thomas, and E. P. Turtle, LROC - Lunar Reconnaissance Orbiter Camera, Lunar and Planetary Science XXXVI, Extended Abstract No. 1576, Lunar and Planetary Institute, Houston, Texas, 2005.
21. Rosiek, M. R., Kirk, R., Howington-Kraus, E., Digital Elevation Models Derived from Small Format Lunar Images, ASPRS 2000.

22. Tooley, C., 2006. LRO Spacecraft and Objectives.
URL: <http://lunar.gsfc.nasa.gov> (last date accessed: Nov. 12, 2009).
23. USGS Isis, 2009. URL: <http://isis.astrogeology.usgs.gov> (last date accessed: Nov. 12, 2009).
24. Watzin, J.G., Joseph Burt, and Craig Tooley 2005. The Robotic Lunar Exploration Program (RLEP) – An Introduction to the Goals, Approach, and Architecture. American Institute of Aeronautics and Astronautics.
25. Wolf, P. R., 1983. Elements of Photogrammetry, second edition, McGRAW-Hill international editions.